

An Improved Fingerprint Method for Indoor Mobile Object Positioning

Prima Kristalina^{a,*}, Syafira S. Salsabila^a, Rafina D. Ainul^b, Musayyanah^c, Afifah D. Ramadhani^a

^a Department of Electrical Engineering, Politeknik Elektronika Negeri Surabaya, Surabaya, 60111, Indonesia

^b Department of Informatics, Universitas Surabaya, Surabaya, 60293, Indonesia

^c Department of Computer Engineering, Universitas Dinamika, Surabaya, 60298, Indonesia

Corresponding author: *prima@pens.a.c.id

Abstract— The mobility of people in big cities tends to increase with the improvement in the availability of sharing access in public facilities. However, the dense environment with moving objects will allow the possibility of the object's detachment from a monitoring system. This condition will cause concern, especially if the object is a priority that needs to be protected. We propose a system for detecting moving objects in indoor environments using a fingerprint method of Received Signal Strength (RSSI) data retrieval. The work was conducted in the observation area, a part of a mall full of tenant stores and humans moving during shopping hours. The randomness of RSSI data emitted from access points in the indoor area is affected by multipath and signal reflection because of walls or furniture existing in the building. The K-NN regression algorithm was utilized to generate RSSI data based on the on-site measurement to prune this randomness. The generated data will be clustered, using the K-means algorithm and Elbow method to ensure the optimal number of K. The experiment results showed that using the best K for RSSI clustering, the positioning accuracy produced by the system reached 77% of the total expected accuracy. Meanwhile, according to the signal characteristics of indoor buildings, the entrance corner had the worst data distribution, with 37.35% of the data generated having an RSSI value close to the receiver sensitivity threshold.

Keywords— Indoor positioning; received signal strength; K-NN regression; fingerprint.

Manuscript received 27 Oct. 2022; revised 7 Nov. 2022; accepted 24 Jan. 2023. Date of publication 30 Jun. 2023.
IJASEIT is licensed under a Creative Commons Attribution-Share Alike 4.0 International License.



I. INTRODUCTION

The presence of moving objects in a crowded center is an interesting trend to be studied. The sharing of access to public facilities or recreational needs causes the formation of human groups within indoor environments, such as in train stations, airports, hospitals, malls, and so on. A crowded situation in public facilities will cause objects to be detached from monitoring, especially if the object is a priority that needs to be taken care of, such as children, the elderly, or prisoners. Detection and tracking of humans or moving objects in dense environments must be considered [1]–[3]. Various studies for the detection of human activities in dense environments usually use images as input data for the detection of faces or bodies [2], [4], [5]. However, sending image data to the server usually uses a wired network because of the large size of the image data.

Tracking the activities of moving objects in the indoor field has been widely proposed to monitor the movement of objects

around the observation area [6]–[8]. Various studies on using RSSI offer interesting ideas for sending data wirelessly [9]–[13]. The received signal data is sufficiently obtained from the activation of hotspots/access points that are widely found in public indoor spaces that can be used by the public. The signal strength data is received by the user's smartphone connected to the hotspot. This received signal data is processed with several machine learning-based detection and optimization methods [14], [15] as well as filtering methods [16], [17] to obtain the best position estimation accuracy.

Moreover, the K-NN algorithm has been widely proposed for improving position estimation in an indoor area [18], [19], which aims to classify the input data of sensors in wireless networks to obtain optimal position estimation. Similarly, the clustering method with K-means has also been proposed by some researchers [15], [20] to categorize the observation areas based on their path loss coefficients to process the objects' localizing easily. The fingerprinting method is widely used in managing received signal data in object localization

techniques. This method has proven effective in obtaining accurate position estimates with the availability of a huge data that can be processed. Thus the position estimation error can be kept to a minimum [21]–[24].

This work proposes the RSSI clustering method in an indoor area. The fingerprint method was conducted to retrieve the initial received signal data. This method divides the data into offline phase and online phase data for further processing in determining the estimated position of the object. The contributions of our proposed work to improve the fingerprint method for indoor mobile object positioning are as follows:

- Employs the K-Nearest Neighbors (K-NN) Regression algorithm for offline data generation so as the amount of received signal data obtained is significant enough to be classified based on the strength of the signal received from each access point in the observation area
- Enhances the K-means algorithm with the Elbow method to ensure the optimal k value to be recommended value of cluster data received from each access point.
- Integrating the entire process, including the collection of received signal data, the data processing, and the determination of the position of the object being sought, into an application that the user will access.

II. MATERIALS AND METHOD

This section divides into three stages: the system design and data preparation, the formation of data clustering and localization, and the implementation of the object detection process into an application. The three stages will be described sequentially in the next subsection.

A. System Design and Data Preparation

The system design includes the backend and frontend parts. The task of the backend is classifying data based on its closest cluster and providing decisions to determine the estimated position of objects based on the results of data clustering. This section is solved with Python programming language. Meanwhile, the front end serves as an application users use to interact with the system in the search for moving objects. The Flutter framework is used to accomplish this part. Moreover, we use Firebase databases to process and store received signal data from offline phase measurements. The illustration of the proposed system is shown in Fig. 1. The Android-based application, namely MyTect, is carried by users who have been registered with it. When the user is in the center of the crowd area that has been confirmed in the system database, the application can be run to search for objects that move around the center of the crowd without activating the GPS.

The initial stage of the work is the preparation of data. Data was collected from the observation area in the form of Wi-Fi Received Signal Strength (RSSI) data. The data was obtained from the receiver (Rx) and the connected Access Point (Tx). The specifications of the observation area are shown in Table 1, while the placement of the Wi-Fi signal reception point in the observation area is shown in Fig. 2.

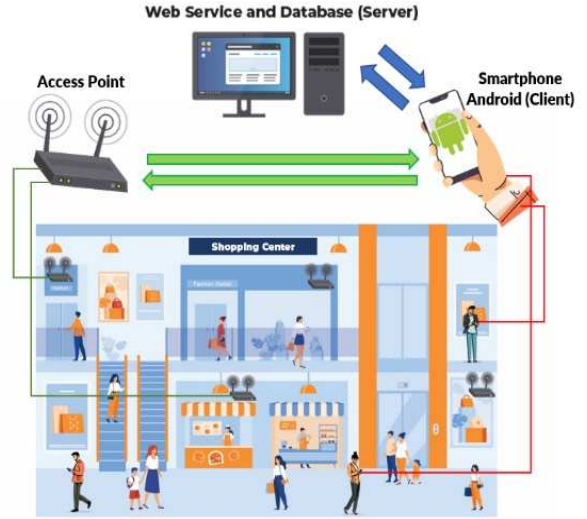


Fig. 1 The proposed system illustration

TABLE I
THE SPECIFICATION OF OBSERVATION AREA

Parameter	Specification
The observation area size	61.6x92.5x m ² (17x25 grid)
Measurement points	232
Access Points	6
Grid space	3.62m
Initial RSSI number	6593



Fig.2 (a). Grid point in observation area; (b). Physical observation area

From hundreds of active hotspots in the observed building, we filtered only 6 Access Points on the 1st floor, where the measurement process was conducted. The specifications of the 6 Access Points are shown in Table 2. We use the fingerprint method to collect the required signal strength data. The signal data emitted from several access points (AP) scattered in the observation field were received at certain points in the area using a Mobile Unit (MU). The RSSI and measurement point data were stored in the database. The data stored was in the form of RSSI values ($RSSI_i$) received at the coordinates (x_i, y_i) of each observation point, i . These data were taken in two phases, i.e., the offline phase, where the data retrieval prior to the object detection process was carried out, and the online phase, where the object detection process was conducted [21], [25], [26]. The illustration of the fingerprint process is shown in Fig. 3.

TABLE II
THE PROFILE OF ACCESS POINTS

level	BSSID	Timestamp	SSID name	Alias	label-ID
-85	68:cc:6e:a3:a5:63	1488115894	TRANSMAR T@WIFI.ID	ssid0	28
-77	68:cc:6e:a3:ae:c0	1508200800	@wifi.id	ssid1	201
-60	68:cc:6e:a3:af:42	1528247197	seamless@wifi.id	ssid2	143
-56	a8:bd:27:ff:9e:60	1548218665	WLAN51	ssid3	46
-71	68:cc:6e:a3:aa:c0	1548219059	@wifi.id	ssid4	46
-84	68:cc:6e:a3:a8:02	1548219099	seamless@wifi.id	ssid5	46

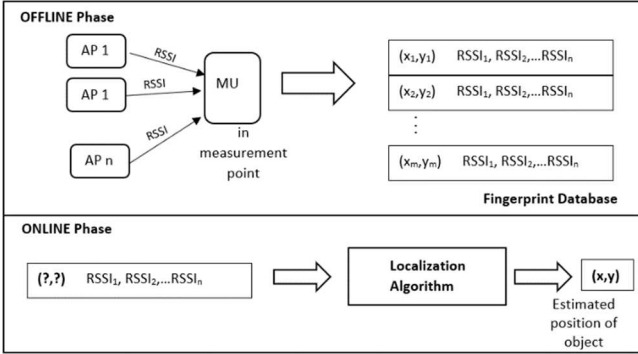


Fig. 3 Two phases of the fingerprint method

Generally, the fingerprint localization method does not require complex calculations. This method simply compares the strength of the signal received in the online phase with the strength of the signal that has been stored in the database measured in the offline phase. The coordinate of the measurement point i (at offline phase) will be the estimated position from the object (at online phase) that obtained the similar or closest signal with the signal strength on the coordinate of the point i , i.e. (x_i, y_i) [24], [27], [28].

In this work, we generated additional data in the offline phase, intending to obtain more prediction RSSI data and the position of observation points. The more the number of offline data available, the more it is hoped that it will minimize the position estimation error of the online data. The initial area of each grid was 17×25 grids will be reduced to half, thus obtaining a larger number of grids, which was 34×50 grids. The purpose of adding this grid is to increase the amount of RSSI prediction data. The K-Nearest Neighbor Regression method is used for data generation. The initial measurement data is divided into 80% training data and 20% testing data. K-NN Regression is widely used for the prediction of sensor data on wireless sensor networks, due to its lightweight computing, with data prediction values that have fairly good accuracy [18], [29], [30]. Each training data and test data differed according to the feature (distance) and label (signal strength). The feature is the distance between the coordinates of the measurement point to the coordinates of each SSID, while the label is the strength of the signal measured at that point. The feature values are expressed in Equation (1)

$$D_{ij} = \sqrt{(x_i - x_j)^2 + (y_i - y_j)^2} \quad (1)$$

where (x_i, y_i) is the coordinate of measurement point i , and (x_j, y_j) is the coordinate of Access Point or SSID j . In the same way, select the feature measurements for predefined observation point targets when the number of grid sizes was increased. Furthermore, with K-NN regression, get the average Euclidean distance of the target to obtain the closest label to the feature, as expressed in Equation (2), where z_L and z_j are the coordinate of the new measurement points L and j respectively. The algorithm of the comprehensive process is shown in Algorithm 1.

$$\bar{D}_{jL} = \frac{1}{k} \sum_{L=1}^m |z_L - z_j| \quad (2)$$

Algorithm 1. K-NN Regression for Data Generation in offline phase

Input:

$A = \{x_1, x_2, \dots, x_n\}$ // Set of initial RSSI

$B = \{z_1, z_2, \dots, z_n\}$ // Set of initial reference point's coordinates

$Z = \{z_1, z_2, \dots, z_m\}$ // Set of new reference point's coordinates

Output:

$Y = \{y_1, y_2, \dots, y_m\}$ // Set of new RSSI

1. **For** each SSID
2. Sort data
3. Divide initial data into 80% training data and 20% testing data
4. **For** each training data
5. Calculate the distance between the reference point's coordinate and SSID's coordinate, d_{si}
6. Save data label, distance d_{si} and RSSI _{i}
7. **End** for training data
8. Examine the testing data
9. Double the grid size of observation area
10. Repeat step 4 to 7
11. Select k closest distance d_{sj} and RSSI _{j}
12. Output the mean of z_j
13. **End** for

By implementing the K-NN Regression, we will generate a larger amount of data according to the number of enlarged grid points, which is 34×50 against the 6 available SSIDs, which will result in as many as 10200 data. The results of generating RSSI data against the distance between observation points and each SSID using K-NN regression are shown in Fig. 4.

B. Data Clustering and Localization

The RSSI clustering was carried out on each SSID to facilitate the localization process in the online phase of the fingerprint method. We used the K-Means algorithm to undertake this process. The advantage of K-means is its computational speed in data grouping. Therefore, the K-means algorithm is sufficient for the clustering process of RSSI data in indoor positioning where the RSSI value varies greatly. [15], [20], [30].

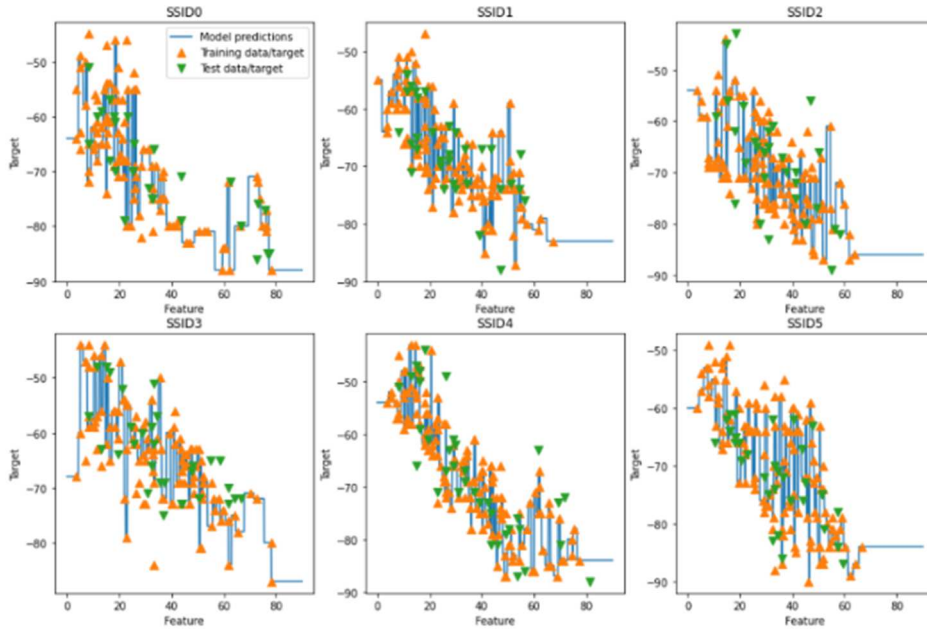


Fig. 4 Plot of training and testing data for each SSID

To ensure the appropriate K value to be used in the K-means algorithm, we added the Elbow method, i.e. a method used to produce information in shaping the optimal number of clusters. In this method, the K-means algorithm was run with the number of K that has been determined randomly, then the centroid of each cluster was decided. Compute the distance among measurement points towards its centroid, then plot it on a graph. The graph where the curve is angular (down quickly from the previous condition), has the most optimal K value. The determination of K is executed by evaluating the inertia of the cluster or the Sum of Squared Error (SSE), concerning the center/centroid as shown in Equation (3)

$$SSE = \sum_{k=1}^m \sum_{i=1}^n |x_i - c_k| \quad (3)$$

where x_i is an i^{th} data object, and c_k is a centroid data of k^{th} cluster. The K-means algorithm is supported by the Elbow method to ensure the appropriate number of K in the RSSI clustering is given in Algorithm 2. Using the K-means clustering, we obtained RSSI data groups labeled according to the closest SSID. Some of the results of clustering are shown in Table 3.

Algorithm 2 K-means for RSSI clustering

Input:

$A = \{x_1, x_2, \dots, x_n\}$ // Set of RSSI

Output:

Y //Set of RSSI of each cluster

1. Specify the number of K of cluster to assign, use Elbow method to ensure the number of K
 2. Randomly initiate k centroids
 3. **Repeat**
 4. **expectation:** assign each point to its closest centroid
 5. **maximization:** calculate the new centroid (mean) for each cluster
 6. **Until** the centroid position does not change
-

TABLE III
CLUSTER-BASED RSSI FOR EACH SSID

No.	Level ssid0	cluster ssid1	Level ssid1	cluster ssid1	Level ssid2	cluster ssid2	Level ssid3	cluster ssid3	Level ssid4	cluster ssid4	Level ssid5	cluster ssid5
0	-80	3	-74	3	-62	0	-55	0	-68	2	-76	2
1	-60	0	-69	2	-75	3	-74	3	-79	3	-73	2
2	-79	3	-70	2	-62	0	-56	0	-68	2	-72	2
3	-60	0	-63	1	-75	3	-73	3	-79	3	-71	2
...
1693	-79	3	-74	3	-76	3	-72	3	-65	1	-58	0
1694	-75	2	-74	3	-77	3	-74	3	-79	3	-70	2
1695	-79	3	-74	3	-76	3	-73	3	-66	2	-58	0
1696	-80	3	-74	3	-76	3	-69	2	-52	0	-67	1
1697	-80	3	-75	3	-76	3	-68	2	-53	0	-70	2
1698	-80	3	-75	3	-76	3	-68	2	-53	0	-72	2
1699	-80	3	-75	3	-76	3	-68	2	-57	0	-75	2

The coordinates and RSSI data obtained from shifting objects in the examination area were sent to the backend server in the localization process. The data will be matched to the RSSI data and the distance of the offline measurement results that have been clustered previously. The offline measurement data with the closest Euclidean distance will be the estimated position of the moving object. The accuracy value of the estimated position results was analyzed based on the estimation error value obtained during testing to the total data, as depicted in Equation (4).

$$accuracy = \frac{(N-E)}{N} \times 100\% \quad (4)$$

where N is the amount of measurement and E is the amount of error estimation. Once the object moves from the initial point to the next point, the localization process will be repeated. The repeated process will be conducted consecutively until the object leaves the observation area. The estimated position of moving objects in the building will always be reported through an application brought by the user that has the object's responsibility in real-time.

C. Implementation of the System

The object detecting and positioning will be implemented in the application system, named MyTect. This application has several menus: the home menu, simulation, people, history, and profile. The home menu was used to scan and input training data for the offline fingerprint database obtained from the access point, the simulation menu performed simulations in determining the estimated user position, the people menu was used to monitor the position of other users, the history menu provided the training data that has been recorded to the database, and the profile menu was used to view the user profile.

The application is opened with a splash screen that displays the logo, then enters the login page. Once the user successfully signed in, the home menu appeared. This menu displayed information related to the RSSI value and the location of the observation area. To monitor the position of others, the user should open the people menu. This menu provided a list of other users position who has previously estimated their position. The menu will display a picture of the place and the name of the user who was looked for. The part of the application's display is shown in Fig. 5.



Fig. 5 Application Mockup: a) Splash Screen; b) Received signal from the adjacent SSID; c) Monitoring the other's position

The results of the system evaluation will be presented in this section, including an evaluation and discussion of the K-NN regression method for generating auxiliary RSSI data in the offline phase, the use of the K-means algorithm with the supported Elbow method for the offline data clustering process, and the examination of the localization accuracy processed with the fingerprint method.

A. K-NN Regression for RSSI data on Offline Phase

The initial measurement data were still too few to be used as training and testing data. For this reason, we generated new data using the K-NN regression method [31] by doubling the size grid size in the observation area to produce 10200 data from 1700 grid points. This was almost twice as large as the previous amount of data, with 6593 data from 232 grid points. Based on the K-NN regression model from the training data and data set in Fig. 3, the RSSI distribution from several corners in the observation area, namely the Sports corner, Food Material corner, and home living corner, has been obtained. Several K values have been selected for each corner to retrieve the best RSSI distribution from the SSID. The value of K was 20, 23, and 30, respectively.

In the sports corner area, 9 measurement points were selected (representing more than 20 measurement points). Based on several examinations with various K values, it was found that the largest signal strength given by SSID 3 with an average of RSSI was -64 dBm, while the weakest signal strength given by SSID 5 with an average of RSSI was -76 dBm. The unity of K determined the density of received signal distribution σ . Using K=20, 23, and 30 the SSID 5 provided deviation standards $\sigma = 1.03, 0.95, \text{ and } 0.89$, respectively. Meanwhile, SSID 3 provided $\sigma = 1.99, 1.85, \text{ and } 1.74$ for those K values. Thus, the larger the value of K, the denser the distribution of the received signal strength data. However, it does not guarantee that the greater the value of K, the better the received signal strength because there is the possibility that the distribution of data in the wrong value range will also be greater.

In associated with the position of the SSIDs towards the position of each corner, the largest signal strength received by the device in the Sports corner should be from SSID 0 (see Fig. 2a). Due to this discrepancy, we examined deeply the error signal strength received from SSID 0 using a Pareto diagram. From 1700 signal strength data received from SSID 0, we mapped the occurrence frequency of the RSSI to find the largest value that caused the error. Fig. 6 shows a Pareto diagram of the received signal strength distribution from SSID 0. It can be seen that the largest occurrence frequency is RSSI data with a range of -80.3 to -78 dBm, where the percentage of the total occurrence of the total amount of data is $(635/1700) \times 100\% = 37.35\%$. On the other hand, 37.35% of RSSI data from SSID 0 with a range of -80.3 to -78 dBm were received by 1700 points spread out in the observation area. This RSSI value was close to the receiver sensitivity threshold, meaning that these are bias values, not the correct RSSI values. This situation occurred because physically SSID 0 was installed near the entrance of the building, where the signal from the SSID itself was already polarized outside the observation area. Consequently, the

measurement results in such points near this SSID yield biased values.

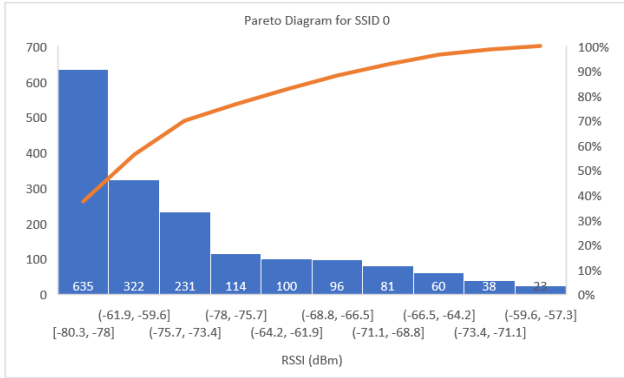
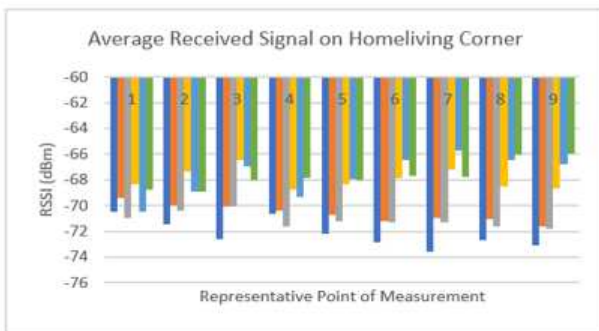
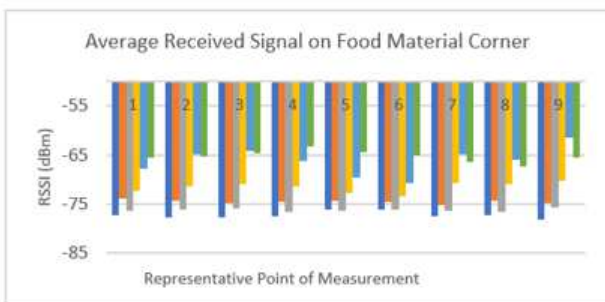


Fig. 6 Pareto Diagram for Received Signal Data Distribution from ssid0

Besides the sports corner, the average received signal strength at the food material corner and home living corner from the 6 SSIDs was analyzed as well. The largest signal strength in the home living was obtained from ssid5 of -67.65 dBm on average, and the smallest was from ssid0 of -72.2 dBm, as seen in Fig. 7(a). On the other hand, the largest signal strength in the food material corner came from ssid4 with an average of -65 dBm, and the weakest was from ssid0 with -77.3 dBm, as seen in Fig. 7(b). This is increasingly convincing that the location of the food material corner is close to ssid4, and home living is close to ssid4 and ssid5.



a)



b)

Fig. 7 Average Received Signal on various Measurement Points: a) Home Living Corner; b) Food Material Corner

Based on the deterministic statistic, the value of the mean, variance, standard deviation, minimum, and a maximum of RSSI transmitted by each SSID to the observation points are shown in Fig. 8. According to the values. The signal strength data was most widely spread in ssid4, where physically, the

position of this access point was at the very end of the building. There was much furniture made of wood and iron. These materials cause absorption and signal reflection, and this process, due to the signal characteristic, causes high randomness received signal strength. With such a large distribution, the signal strength emitted by ssid4 was often received by the surrounding measurement points, even those far from the AP. Therefore, in some corners, ssid4 has the largest signal strength distribution compared to other SSIDs.

	ssid0	ssid1	ssid2	ssid3	ssid4	ssid5
count	1700	1700	1700	1700	1700	1700
mean	-72.24	-69.64	-70.54	-67.23	-70.25	-70.12
STD	7.75	5.49	5.65	6.58	9.36	6.67
variance	59.99	30.14	31.89	43.3	87.85	44.5
min	-80	-76	-77	-75	-80	-82
max	-59	-58	-62	-55	-52	-57

Fig. 8 Statistic Values for each SSID

B. Cluster-based Received Signal data using K-means

In the data clustering process with K-Means, we use the Elbow method considering the severe point of the data drop on the curve. The optimal number of clusters was achieved by examining the SSE (Sum Square Error) from each data range to the centroid with various k values and noticing the point on the graph where the curve can form an elbow [32]. The position where the curve formed an angle indicated the suggested optimal k value. Fig. 9 represents each k's score, while the elbow curve of each SSID is shown in Fig. 10.

SSID	K=2	K=3	K=4	K=5	K=6	K=7
ssid0	0.7526	0.7043	0.7789	0.7652	0.7445	0.7428
ssid1	0.7048	0.7032	0.7363	0.7326	0.7297	0.7308
ssid2	0.7278	0.7159	0.7337	0.7032	0.7049	0.7250
ssid3	0.6415	0.7503	0.7345	0.7392	0.7357	0.7326
ssid4	0.6843	0.7659	0.7508	0.7425	0.7388	0.7502
ssid5	0.6205	0.6313	0.6749	0.6991	0.6812	0.6945

Fig. 9 The K score of Received Data on each SSID

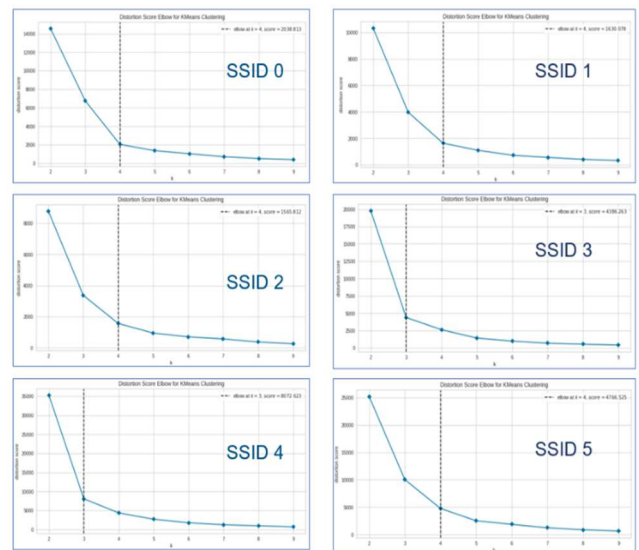


Fig. 10 Elbow Curve for each SSID

The recommended numbers of k and elbow scores for each SSID are given in Table 4. Along with the optimal k obtained by the Elbow method, it is found that the comprehensive RSSI data from ssid0, ssid1, ssid2, and ssid5 will be formed into 4 clusters, while data from ssid3 and ssid4 will be formed into 3 clusters.

TABLE IV
CLUSTER NUMBER AND ELBOW SCORE FOR ALL SSID

SSID	The number of clusters (k)	The Elbow Score
ssid0	4	2038.813
ssid1	4	1630.078
ssid2	4	1565.812
ssid3	3	4386.263
ssid4	3	8072.623
ssid5	4	4766.525

C. The evaluation of Estimated Position Accuracy

In the online phase of the fingerprint, the object moves at a certain point in the observation area. The RSSI received by the object's mobile unit from several Access Points will then be matched with the RSSI data from the closest cluster stored in the database. Furthermore, the recommendation for the current position will be displayed in MyTect application. The decision of position estimation depended on the percentage of error accuracy, calculated based on the percentage of estimated position error to the total number of tests. There were 60 accuracy tests with a "True" score when the estimated position result matches the actual position. On the contrary, the score is "False" if they do not match, as shown in Table 5. This table shows from the total 60 tests, 14 points of them were errors. Thus, the percentage of position accuracy of the system designed was 77%.

TABLE V
THE EVALUATION RESULT OF THE ESTIMATED POSITION

N o.	X	Y	Actual Position	Estimated Position	Status
1	1	25	Cooking	Snacks, Home Appliances, Stationary	False
2	2	25	Cooking	Snacks, Home Appliances, Stationary	False
3	4	6	Soap and skincare	Soap and skincare, Kitchenware	True
4	4	8	Soap and skincare	Soap and skincare Home Appliances, Stationary	True
5	4	25	Cooking	Snacks, Home Appliances, Stationary	False
6	5	25	Cooking	Snacks, Home Appliances, Stationary	False
.
.
.
60	4	13	Snacks	Snacks	True

IV. CONCLUSION

This paper proposes improving the fingerprint method to obtain data homogeneity in an RSSI data cluster. The data will be used to calculate the estimated position of an object that moves indoors. The experiment result shows that there is a large distribution of RSSI data in one of the Access points in the observation area. This situation affects the offline RSSI data clustering process using K-means, even though the K-NN and Elbow methods were explored to assist the K-means in reaching the optimal estimated position of the object.

Consequently, some data are not selected in certain clusters. Therefore, when the matches process between online and offline data using the closest Euclidean distance approach was carried out, the best accuracy could not be obtained. The next work will correct this condition with a more stringent data selection method to get better offline data homogeneity.

REFERENCES

- [1] Z. Zhou, L. Li, A. Fürsterling, H. J. Durocher, J. Mouridsen, and X. Zhang, "Learning-based object detection and localization for a mobile robot manipulator in SME production," *Robot. Comput. Integr. Manuf.*, vol. 73, no. February 2021. doi: 10.1016/j.rcim.2021.102229.
- [2] I. Stolas, S. Suarez, D. Pereyra, F. De Izaguirre, and V. Cabrera, "Human activity recognition using machine learning techniques in a low-resource embedded system," in *2021 IEEE URUCON, URUCON 2021*, 2021. doi: 10.1109/URUCON53396.2021.9647236.
- [3] J. Zhu, Z. Wang, S. Wang, and S. Chen, "Moving object detection based on background compensation and deep learning," *Symmetry (Basel)*, vol. 12, no. 12, 2020, doi: 10.3390/sym12121965.
- [4] A. Zheng, Y. Zhang, X. Zhang, X. Qi, and J. Sun, "Progressive End-to-End Object Detection in Crowded Scenes," in *2022 IEEE/CVF Conference on Computer Vision and Pattern Recognition (CVPR)*, 2022, pp. 847–856. doi: 10.1109/cvpr52688.2022.00093.
- [5] K. Peng, Y. Zhang, W. Gao, and Z. Lu, "Evaluation of human activity intensity in geological environment problems of Ji'nan City," *European Journal of Remote Sensing*, vol. 54, no. sup2. 2021. doi: 10.1080/22797254.2020.1771214.
- [6] C. Chen and D. Li, "Research on the Detection and Tracking Algorithm of Moving Object in Image Based on Computer Vision Technology," *Wirel. Commun. Mob. Comput.*, vol. 2021, 2021, doi: 10.1155/2021/1127017.
- [7] Y. Fu, R. Liu, H. Zhang, G. Liang, S. ur Rehman, and L. Liu, "Continuously tracking of moving object by a combination of ultra-high frequency radio-frequency identification and laser range finder," *Int. J. Distrib. Sens. Networks*, vol. 15, no. 7, 2019, doi: 10.1177/1550147719860990.
- [8] H. Obeidat, W. Shuaib, O. Obeidat, and R. Abd-Alhameed, *A Review of Indoor Localization Techniques and Wireless Technologies*, vol. 119, no. 1. Springer US, 2021. doi: 10.1007/s11277-021-08209-5.
- [9] A. Booranawong, N. Jindapetch, and H. Saito, "A System for Detection and Tracking of Human Movements Using RSSI Signals," *IEEE Sens. J.*, vol. 18, no. 6, pp. 2531–2544, 2018, doi: 10.1109/JSEN.2018.2795747.
- [10] N. Abdul, K. Zghair, M. S. Croock, A. Abdul, and R. Taresh, "Indoor Localization System Using Wi-Fi Technology," *Iraqi J. Comput. Commun. Control Syst. Eng.*, pp. 69–77, 2019, doi: 10.33103/uo.t.ijccce.19.2.8.
- [11] H. Wang, F. Zhang, and W. Zhang, "Human Detection through RSSI Processing with Packet Dropout in Wireless Sensor Network," *J. Sensors*, vol. 2020, 2020, doi: 10.1155/2020/4758103.
- [12] Y. Shi, W. Shi, X. Liu, and X. Xiao, "An RSSI classification and tracing algorithm to improve trilateration-based positioning," *Sensors (Switzerland)*, vol. 20, no. 15, pp. 1–17, 2020, doi: 10.3390/s20154244.
- [13] R. R. Hastari, M. Yuliana, and P. Kristalina, "Students Trajectory Pattern Finding Scheme Based on RSSI Geolocation as a Part of Smart Campus," *Int. Electron. Symp. 2021 Wirel. Technol. Intell. Syst. Better Hum. Lives, IES 2021 - Proc.*, pp. 337–342, 2021, doi: 10.1109/IES53407.2021.9594045.
- [14] J. Chen, X. Huang, H. Jiang, and X. Miao, "Low-cost and device-free human activity recognition based on hierarchical learning model," *Sensors*, vol. 21, no. 7, 2021, doi: 10.3390/s21072359.
- [15] B. Pinto, R. Barreto, E. Souto, and H. Oliveira, "Robust RSSI-based Indoor Positioning System using K-Means Clustering and Bayesian Estimation," *IEEE Sens. J.*, no. July, 2021, doi: 10.1109/JSEN.2021.3113837.
- [16] R. D. Ainul, P. Kristalina, and A. Sudarsono, "Hybrid filter scheme for optimizing indoor mobile cooperative tracking system," *Telkomnika (Telecommunication Comput. Electron. Control)*, vol. 16, no. 6, pp. 2536–2548, 2018, doi: 10.12928/TELKOMNIKA.v16i6.10162.
- [17] C. R. Pratiwi, P. Kristalina, and A. Sudarsono, "A performance evaluation of modified weighted pathloss scenario based on the cluster

- based-PLE for an indoor positioning of wireless sensor network,” *Int. J. Eng. Technol. Innov.*, vol. 9, no. 1, pp. 61–74, 2019.
- [18] R. K. Yadav, B. Bhattarai, H. S. Gang, and J. Y. Pyun, “Trusted K nearest Bayesian estimation for indoor positioning system,” *IEEE Access*, vol. 7, pp. 51484–51498, 2019, doi: 10.1109/ACCESS.2019.2910314.
- [19] A. Javaid *et al.*, “Machine learning algorithms and fault detection for improved belief function based decision fusion in wireless sensor networks,” *Sensors (Switzerland)*, vol. 19, no. 6, pp. 1–28, 2019, doi: 10.3390/s19061334.
- [20] K. F. P. Wye *et al.*, “RSSI-based Localization Zoning using K-Mean Clustering,” *IOP Conf. Ser. Mater. Sci. Eng.*, vol. 705, no. 1, 2019, doi: 10.1088/1757-899X/705/1/012038.
- [21] S. Xia, Y. Liu, G. Yuan, M. Zhu, and Z. Wang, “Indoor fingerprint positioning based on Wi-Fi: An overview,” *ISPRS Int. J. Geo-Information*, vol. 6, no. 5, 2017, doi: 10.3390/ijgi6050135.
- [22] N. Alikhani, V. Moghtadaiee, and S. A. Ghorashi, “Fingerprinting Based Indoor Localization Considering the Dynamic Nature of Wi-Fi Signals,” *Wirel. Pers. Commun.*, vol. 115, no. 2, pp. 1445–1464, 2020, doi: 10.1007/s11277-020-07636-0.
- [23] S. Polak, L., Rozum, T. Slanina, M., Bravenec, T., Fryza, and Pikrakis, “Received Signal Strength Fingerprinting-Based Indoor Location Estimation Employing Machine Learning,” *Sensors*, vol. 21, no. 13, p. 4605, 2021, doi: 10.3390/s21134605.
- [24] A. P. Rahmadini, P. Kristalina, and A. Sudarsono, “Optimization of fingerprint indoor localization system for multiple object tracking based on iterated weighting constant - KNN method,” *Int. J. Adv. Sci. Eng. Inf. Technol.*, vol. 8, no. 3, pp. 998–1007, 2018, doi: 10.18517/ijaseit.8.3.6086.
- [25] J. Zheng, K. Li, and X. Zhang, “Wi-Fi Fingerprint-Based Indoor Localization Method via Standard Particle Swarm Optimization,” *Sensors*, vol. 22, no. 13, pp. 1–16, 2022, doi: 10.3390/s22135051.
- [26] X. min Yu, H. qiang Wang, and J. qiu Wu, “A method of fingerprint indoor localization based on received signal strength difference by using compressive sensing,” *Eurasip J. Wirel. Commun. Netw.*, vol. 2020, no. 1, 2020, doi: 10.1186/s13638-020-01683-8.
- [27] C. Zhang, N. Qin, Y. Xue, and L. Yang, “Received signal strength-based indoor localization using hierarchical classification,” *Sensors (Switzerland)*, vol. 20, no. 4, pp. 1–15, 2020, doi: 10.3390/s20041067.
- [28] P. Dai, Y. Yang, M. Wang, and R. Yan, “Combination of DNN and Improved KNN for indoor location fingerprinting,” *Wirel. Commun. Mob. Comput.*, vol. 2019, 2019, doi: 10.1155/2019/4283857.
- [29] X. Peng, R. Chen, K. Yu, F. Ye, and W. Xue, “An improved weighted k-nearest neighbor algorithm for indoor localization,” *Electron.*, vol. 9, no. 12, pp. 1–14, 2020, doi: 10.3390/electronics9122117.
- [30] S. Liu, R. De Lacerda, and J. Fiorina, “WKNN indoor Wi-Fi localization method using k-means clustering based radio mapping,” *IEEE Veh. Technol. Conf.*, vol. 2021-April, 2021, doi: 10.1109/VTC2021-Spring51267.2021.9448961.
- [31] D. Ferreira, R. Souza, and C. Carvalho, “Qa-knn: Indoor localization based on quartile analysis and the knn classifier for wireless networks,” *Sensors (Switzerland)*, vol. 20, no. 17, pp. 1–22, 2020, doi: 10.3390/s20174714.
- [32] S. S. Salsabila, P. Kristalina, and T. Santoso, “The implementation of Optimal K-Means Clustering for Indoor Moving Object Localization,” *IES 2022 - 2022 Int. Electron. Symp. Energy Dev. Clim. Chang. Solut. Clean Energy Transition, Proceeding*, pp. 210–215, 2022, doi: 10.1109/IES55876.2022.9888517.